TITLE: Identification of Plitidepsin as Potent Inhibitor of SARS-CoV-2-Induced Cytopathic Effect after a Drug Repurposing Screen

AUTHORS: Jordi Rodon[1], Jordana Muñoz-Basagoiti[2,*], Daniel Perez-Zsolt[2,*], Marc Noguera-Julian[2,7], Roger Paredes[2,6], Lourdes Mateu[6], Carles Quiñones[6], Itziar Erkizia[2], Ignacio Blanco[5], Alfonso Valencia[3,4], Víctor Guallar[3,4], Jorge Carrillo[2], Julià Blanco[2,5,7], Joaquim Segalés[8,9], Bonaventura Clotet[2,5,7], Júlia Vergara-Alert[1,+], Nuria Izquierdo-Useros[2,5,+]

*Equal contribution

[+] Dual senior authorship

Corresponding authors: JV-A: julia.vergara@irta.cat and NI-U nizquierdo@irsicaixa.es

Affiliations: [1]IRTA, Centre de Recerca en Sanitat Animal (CReSA, IRTA-UAB), Campus de la UAB, 08193 Bellaterra (Cerdanyola del Vallès), Spain

[2]IrsiCaixa AIDS Research Institute, 08916, Badalona, Spain

[3]Barcelona Supercomputing Center

[4]Catalan Institution for Research and Advanced Studies (ICREA), Barcelona, Spain

[5]Germans Trias i Pujol Research Institute (IGTP), Can Ruti Campus, 08916, Badalona, Spain

[6]Germans Trias i Pujol Hospital, Badalona, Catalonia, Spain

[7]University of Vic–Central University of Catalonia (UVic-UCC), Vic, Spain

[8]UAB, CReSA (IRTA-UAB), Campus de la UAB, 08193 Bellaterra (Cerdanyola del Vallès), Spain

[9]Departament de Sanitat i Anatomia Animals, Facultat de Veterinària, UAB, 08193 Bellaterra (Cerdanyola del Vallès), Spain

ABSTRACT (234)

There is an urgent need to identify therapeutics for the treatment of Coronavirus diseases 2019 (COVID-19). Although different antivirals are given for the clinical management of SARS-CoV-2 infection, their efficacy is still under evaluation. Here, we have screened existing drugs approved for human use in a variety of diseases, to compare how they counteract SARS-CoV-2-induced cytopathic effect and viral replication *in vitro*. Among the potential 72 antivirals tested herein that were previously proposed to inhibit SARS-CoV-2 infection, only 18% had an IC_{50} below 25 µM or 10^2 IU/mL. These included plitidepsin, novel cathepsin inhibitors, nelfinavir mesylate hydrate, interferon 2-alpha, interferon-gamma, fenofibrate, camostat along the well-known remdesivir and chloroquine derivatives. Plitidepsin was the only clinically approved drug displaying nanomolar efficacy. Four of these families, including novel cathepsin inhibitors, blocked viral entry in a cell-type specific manner. Since the most effective antivirals usually combine therapies that tackle the virus at different steps of infection, we also assessed several drug combinations. Although no particular synergy was found, inhibitory combinations did not reduce their antiviral activity. Thus, these combinations could decrease the potential emergence of resistant viruses. Antivirals prioritized herein identify novel compounds and their mode of action, while independently replicating the activity of a reduced proportion of drugs which are mostly approved for clinical use. Combinations of these drugs should be tested in animal models to inform the design of fast track clinical trials.

Keywords: SARS-CoV-2, antivirals, plitidepsin, synergy

INTRODUCTION

A novel betacoronavirus, the severe acute respiratory syndrome coronavirus 2 (SARS-CoV-2), is causing a respiratory disease pandemic that began in Wuhan, China, in November 2019, and has now spread across the world [1]. To date, remdesivir is the only approved antiviral drug for the specific treatment of this coronavirus infectious disease 2019 or COVID-19 [2,3]. However, several drugs are being used in the frontline of clinical management of SARS-CoV-2-infected individuals in hospitals all around the world, to try to avoid the development of the COVID-19 associated pneumonia, which can be fatal. By the end of December 2020, almost 1.7 million people had died from COVID-19, and over 75 million cases have been reported (https://covid19.who.int).

Although different drug regimens are being applied to hospitalized patients, no clinical study has evidenced their efficacy yet. Under this scenario, initiatives launched by the World Health Organization (WHO), such as the SOLIDARITY study that has compared remdesivir, hydroxychloroquine, ritonavir/lopinavir and ritonavir/lopinavir plus ß-interferon regimes, have been of critical importance to prioritize the use of the most active compounds [4]. Unfortunately, although remdesivir has proven efficacy in randomized controlled trials [2,3], a recent update of the WHO clinical trial has failed to detect any effect on overall mortality, initiation of ventilation and duration of hospital stay with any of the antivirals tested [5]. Thus, there is an urgent need to identify novel therapeutic approaches for individuals with COVID-19 developing severe disease and fatal outcomes.

In this report we present a prioritized list of effective compounds with proven antiviral efficacy *in vitro* to halt SARS-CoV-2 replication. Compounds were analyzed depending on their expected mechanism of action, to identify candidates tackling diverse steps of the viral life cycle. SARS-CoV-2 entry requires viral binding and spike protein activation via interaction with the cellular receptor ACE2 and the cellular protease TMPRSS2[6], a mechanism favored by viral internalization via endocytosis. Interference with either of these processes has proven to decrease SARS-CoV-2 infectivity[6,7], and therefore, inhibitors targeting viral entry may prove valuable. In addition, SARS-CoV-2 enters into the cells via endocytosis and accumulates in endosomes where cellular cathepsins can also prime the spike protein and favor viral fusion upon cleavage [6,8,9], providing additional targets for antiviral activity. Once SARS-CoV-2 fuses with cellular

membranes, it triggers viral RNA release into the cytoplasm, where polyproteins are translated and cleaved by proteases [10]. This leads to the formation of an RNA replicase-transcriptase complex driving the production of several negative-stranded RNA via both replication and transcription [10]. Numerous negative-stranded RNAs transcribe into messenger RNA genomes, allowing for the translation of viral nucleoproteins, which assemble in viral capsids at the cytoplasm [10]. These capsids then bud into the lumen of endoplasmic reticulum (ER)-Golgi compartments, where viruses are finally released into the extracellular space by exocytosis. Potentially, any of these viral cycle steps could be targeted with antivirals, so we have thus searched for these compounds as well.

Finally, as the most effective antiviral treatments are usually based on combined therapies that tackle distinct steps of the viral life cycle, we also tested the active compounds in combination. These combinations may be critical to abrogate the potential emergence of resistant viruses and to increase antiviral activity, enhancing the chances to improve clinical outcome.

MATERIAL & METHODS

Ethics statement. The institutional review board on biomedical research from Hospital Germans Trias i Pujol (HUGTiP) approved this study. The individual who provided the sample to isolate virus gave a written informed consent to participate.

Cell Cultures. Vero E6 cells (ATCC CRL-1586) were cultured in Dulbecco's modified Eagle medium, (DMEM; Lonza) supplemented with 5% fetal calf serum (FCS; EuroClone), 100 U/mL penicillin, 100 µg/mL streptomycin, and 2 mM glutamine (all ThermoFisher Scientific). HEK-293T (ATCC repository) were maintained in DMEM with 10% fetal bovine serum, 100 IU/mL penicillin and 100 µg/mL streptomycin (all from Invitrogen). HEK-293T overexpressing the human ACE2 were kindly provided by Integral Molecular Company and maintained in DMEM (Invitrogen) with 10% fetal bovine serum, 100 IU/mL penicillin and 100 µg/mL streptomycin, and 1 µg/mL of puromycin (all from Invitrogen). TMPRSS2 human plasmid (Origene) was transfected using X-tremeGENE HP Transfection Reagent (Merck) on HEK-293T overexpressing the human ACE2 and maintained in the previously described media containing 1 mg/ml of geneticin (Invitrogen) to obtain TMPRSS2/ACE2 HEK-293T cells.

Virus isolation, titration and sequencing. SARS-CoV-2 was isolated from a nasopharyngeal swab collected from an 89-year-old male patient giving informed consent and treated with Betaferon and hydroxychloroquine for 2 days before sample collection. The swab was collected in 3 mL medium (Deltaswab VICUM) to reduce viscosity and stored at -80ºC until use. Vero E6 cells were cultured on a cell culture flask (25 cm^2) at 1.5 x 10^6 cells overnight prior to inoculation with 1 mL of the processed sample, for 1 h at 37ºC and 5% CO_2. Afterwards, 4 mL of 2% FCS-supplemented DMEM were supplied and cells were incubated for 48 h. Supernatant was harvested, centrifuged at 200 x g for 10 min to remove cell debris and stored at -80ºC. Cells were assessed daily for cytopathic effect and the supernatant was subjected to viral RNA extraction and specific RT-qPCR using the SARS-CoV-2 UpE, RdRp and N assays [11]. The virus was propagated for two passages and a virus stock was prepared collecting the supernatant from Vero E6.

Viral RNA was extracted directly from the virus stock using the Indimag Pathogen kit (Indical Biosciences) and transcribed to cDNA using the PrimeScript™ RT reagent Kit

(Takara) using oligo-dT and random hexamers, according to the manufacturer's protocol. DNA library preparation was performed using SWIFT amplicon SARS-CoV-2 panel (Swift Biosciences). Sequencing ready libraries where then loaded onto Illumina MiSeq platform and a 300bp paired-end sequencing kit. Sequence reads were quality filtered and adapter primer sequences were trimmed using trimmomatic. Amplification primer sequences were removed using cutadapt [12]. Sequencing reads were then mapped against coronavirus reference (NC_045512.2) using bowtie2 tool [13]. Consensus genomic sequence was called from the resulting alignment at a 18x1800x879 average coverage using samtools [14]. Genomic sequence was deposited at GISAID repository (http://gisaid.org) with accession ID EPI_ISL_510689.

Pseudovirus production. HIV-1 reporter pseudoviruses expressing SARS-CoV-2 Spike protein and luciferase were generated using two plasmids. pNL4-3.Luc.R-.E- was obtained from the NIH AIDS repository. SARS-CoV-2.SctΔ19 was generated (Geneart) from the full protein sequence of SARS-CoV-2 spike with a deletion of the last 19 amino acids in C-terminal, human-codon optimized and inserted into pcDNA3.4-TOPO [15]. Spike plasmid was transfected with X-tremeGENE HP Transfection Reagent (Merck) into HEK-293T cells, and 24 hours post-transfection, cells were transfected with pNL4-3.Luc.R-.E-. Supernatants were harvested 48 hours later, filtered with 0.45 µM (Millex Millipore) and stored at -80ºC until use. Control pseudoviruses were obtained by replacing the spike plasmid by a VSV-G plasmid (kindly provided by Dr. Andrea Cimarelli). The $p24^{gag}$ content of all viruses was quantified using an ELISA (Perkin Elmer) and viruses were titrated in HEK-293T overexpressing the human ACE2.

Antivirals & compounds. The complete list of compounds used for this study and vendors are shown in Supplementary Tables 1 to 5. Drugs were used at concentrations ranging from 100 µM to 0.0512 nM at 5-fold serial dilutions. NPOs were used at concentrations ranging from 10 µM to 0.00512 nM at 5-fold serial dilutions. Plitidepsin was also assayed at concentrations ranging from 10 µM to 0.5 nM at 3-fold dilutions. Interferons were assayed at concentrations ranging from 10^4 to 0.0005 IU/ml at 5-fold serial dilutions. When two drugs were combined, each one was added at a 1:1 molar ratio at concentrations ranging from 100 µM to 0.0512 nM at 5-fold serial dilutions. In

combination with other drugs, plitidepsin was also assayed at concentrations ranging from 10 µM to 0.5 nM at 3-fold dilutions.

Antiviral activity. Increasing concentrations of antiviral compounds were added to Vero E6 cells and immediately after, we added $10^{1.8}$ TCID50/mL of SARS-CoV-2, a concentration that achieves a 50% of cytopathic effect. Untreated non-infected cells and untreated virus-infected cells were used as negative and positive controls of infection, respectively. To detect any drug-associated cytotoxic effect, Vero E6 cells were equally cultured in the presence of increasing drug concentrations, but in the absence of virus. Cytopathic or cytotoxic effects of the virus or drugs were measured 3 days after infection, using the CellTiter-Glo luminescent cell viability assay (Promega). Luminescence was measured in a Fluoroskan Ascent FL luminometer (ThermoFisher Scientific).

IC_{50} calculation and statistical analysis. Response curves of compounds or their mixes were adjusted to a non-linear fit regression model, calculated with a four-parameter logistic curve with variable slope. Cells not exposed to the virus were used as negative controls of infection, and were set as 100% of viability to normalize data and calculate the percentage of cytopathic effect. Statistical differences from 100% were assessed with a one sample t test. All analyses and figures were generated with the GraphPad Prism v8.0b Software.

In silico drug modeling. We performed Glide docking using an in-house library of all approved drug molecules on the 3CL protease of SARS-CoV-2. For this, two different receptors were used, the 6LU7 pdb structure, after removing the covalently bound inhibitor, and a combination of two crystals from the Diamond collection (https://www.diamond.ac.uk/covid-19). Receptors were prepared with the Schrodinger's protein wizard and Glide SP docking was performed with two different hydrogen bond constraints: Glu16 and His163 (with epsilon protonation); we enforced single constraints and also attempted the combination of both. The best 11 molecules, based on Glides's docking score were selected. Top docking scores, however, did not exceed -9, indicating poor potential binding.

Pseudovirus assay. HEK-293T overexpressing the human ACE2 and TMPRSS2 were used to test antivirals at the concentrations found to be effective for SARS-CoV-2 without toxicity, which were the following: 5 µM for niclosamide; 10 µM for chloroquine, chlorpromazine, ciclesonide, MDL 28170 and fenofibrate; 20 µM for hydroxychloroquine, CA-074-Me and arbidol HCl; 25 µM for E-64d; 50 µM for Baricitinib; 100 µM for Amantadine, NB-DNJ, 3' sialyl-lactose Na salt, Tofacitinib, and Camostat mesylate; 1000 µM for methyl-β-cyclodextrin, and 12,5 mg/ml for AAT. A constant pseudoviral titer was used to pulse cells in the presence of the drugs. At 48h post-inoculation, cells were lysed with the Glo Luciferase system (Promega). Luminescence was measured with an EnSight Multimode Plate Reader (Perkin Elmer).

SARS-CoV-2 detection in the supernatant of infected cells. Viral accumulation in the supernatant of Vero E6 cells infected as described previously in the presence of increasing concentrations of the indicated antiviral compounds was measured at day 3 post-infection. The amount of SARS-CoV-2 nucleoprotein released to the supernatant was measured with an ELISA (SinoBiologicals), according to the manufacturer's protocol.

RESULTS

We have tested the antiviral activity of different clinically available compounds and their combinations by assessing their ability to inhibit viral induced cytopathic effect *in vitro*. Our strategy was circumscribed mostly to compounds approved for clinical use, since they are ideal candidates for entering into fast track clinical trials. Drug selection criteria first focused on compounds already being tested in clinical trials, along with well-known human immunodeficiency virus-1 (HIV-1) and hepatitis C virus (HCV) inhibitors, as well as other compounds suggested to have potential activity against SARS-CoV-2 in molecular docking analysis or *in vitro* assays.

We first assessed the activity of 16 compounds with hypothetical capacity to inhibit viral entry, and then we focused on 22 drugs thought to block viral replication upon SARS-CoV-2 fusion. Molecular docking studies provided an additional 11 candidates, which were predicted to inhibit the SARS-CoV-2 main protease. Finally, 23 compounds with unknown mechanism of action were also assessed. By these means, we have compared 72 drugs and 28 of their combinations for their capacity to counteract SARS-CoV-2-induced cytopathic effect *in vitro.*

1. Antiviral activity of compounds that potentially inhibit viral entry

We first tested compounds that could have an effect before viral entry by impairing virus-cell fusion (**Supp. Table 1**). We confirmed the inhibitory effect of hydroxychloroquine against SARS-CoV-2-induced cellular cytotoxicity on Vero E6 cells [16]. As shown in **Fig. 1A**, this drug was able to inhibit viral-induced cytopathic effects at concentrations where no cytotoxic effects of the drug were observed, as previously reported[16,17]. Since hydroxychloroquine was first administered in combination with the antibiotic azithromycin [22], which induces antiviral responses in bronchial epithelial cells [23], we tested this antibiotic alone and in combination (**Fig. 1A**), but found a similar activity to that of the chloroquine derivative alone (**Fig. 1A**). Indeed, this was also the case when we tested hydroxychloroquine in combination with different HIV-1 protease inhibitors and other relevant compounds currently being tested in clinical trials (**Supp. Table 2**).

Additional Food and Drug Administration (FDA)-approved compounds previously used to abrogate viral entry via clathrin-mediated endocytosis such as amantadine or

chlorpromazine were also tested in this SARS-CoV-2-induced cytotoxicity assay (**Supp. Table 1**). Yet, we did not find any prominent effect of these agents; only a partial inhibition at 100 μM for amantadine (**Fig. 1B**). The broad cathepsin B/L inhibitor E64-d also showed partial inhibitory activity (**Fig. 1B**). E64-d exerts activity against viruses cleaved by cellular cathepsins upon endosomal internalization, as previously described using pseudotyped SARS-CoV-2[6]. While these results could not be confirmed using the specific cathepsin B inhibitor CA-074-Me due to drug-associated toxicity (**Supp. Table 1**), none of these cathepsin inhibitors is approved for clinical use. It has also been suggested that hydroxychloroquine could block SARS-CoV-2 spike interaction with GM1 gangliosides [28]. GM1 gangliosides are enriched in cholesterol domains of the plasma membrane and have been previously shown to bind to SARS-CoV spike protein [29]. This mode of viral interaction is aligned with the capacity of methyl-beta cyclodextrin, which depletes cholesterol from the plasma membrane to abrogate SARS-CoV-2 induced cytopathic effect (**Fig. 1B**), as previously reported for SARS-CoV [29]. Removal of cholesterol redirected ACE2 receptor to other domains, but did not alter the expression of the viral receptor [29]. Moreover, NB-DNJ, an inhibitor of ganglioside biosynthesis pathway, also decreased SARS-CoV-2 cytopathic effect (**Fig. 1B**). These results highlight the possible role of gangliosides in viral binding, although in soluble competition the polar head group of GM3 ganglioside (3' Sialyllactose) was not able to reduce viral-induced cytopathic effect (**Supp. Table 1**). Of note, previously reported antiviral agents such as the autophagy BECN1-stabilizing compounds niclosamide or ciclesonide[30],[31], the membrane lipid intercalating compound arbidol[32] and the two JAK inhibitors baricitinib and tofacitinib[34,35] failed to protected Vero E6 cells from SARS-CoV-2 induced cytopathic effect (**Supp. Table 1**). We next tested camostat, a serine protease inhibitor with capacity to abrogate SARS-CoV-2 Spike priming on the plasma membrane of human pulmonary cells and avoid viral fusion [6]. Camostat showed no antiviral effect on Vero E6 cells (**Fig. 1C**), what indicates that the alternative viral endocytic route is the most prominent entry route in this renal cell type. A broader cellular protease inhibitor such as alpha-1 antitrypsin (AAT), used to treat severe AAT human deficiency and currently under clinical study for COVID-19 due to its anti-inflammatory potential, has already shown capacity to limit SARS-CoV-2 entry in cells expressing TMPRSS2 [36,37]. When we tested AAT antiviral efficacy on Vero E6, AAT exerted an effect but required high concentrations that will most likely rely on the activity of these proteases in the endosomal route (**Fig. 1C**).

To confirm that identified compounds listed in **Supp. Table 1** specifically inhibit the viral entry step, we employed a luciferase-based assay using pseudotyped lentivirus expressing the spike protein of SARS-CoV-2, which allows to detect viral fusion on HEK-293T cells transfected with ACE2. As a control, we used lentiviruses pseudotyped with a VSV glycoprotein, where no entry inhibition above 20% was detected for any of the drugs tested (data not shown). In sharp contrast, SARS-CoV-2 pseudoviruses were effectively blocked by most of the drugs previously tested on Vero E6 with wild-type virus (**Fig. 1D**). The main differences were observed with CA-074-Me, ciclesonide and arbidol. These compounds showed a partial blocking effect on ACE2 HEK-293T cells that was not obvious when using replication competent SARS-CoV-2 on Vero E6 (**Supp. Fig. 1**). In addition, NB-DNJ failed to block viral entry (**Fig. 1D**). Overall, using alternative SARS-CoV-2 viral systems, we could identify chloroquine derivatives, cathepsin inhibitors and cholesterol depleting agents as the most promising candidates to block SARS-CoV-2 endocytosis in Vero E6 and HEK-293T cells transfected with ACE2. However, chloroquine derivatives were the only ones that displayed an IC_{50} below 25 µM (**Table 1**), and were also active abrogating pseudoviral entry into HEK-293T cells expressing ACE2 (**Fig. 1E**). Although camostat failed to inhibit viral fusion on ACE2 HEK-293T cells (**Fig. 1E**), its activity was rescued when these cells were transfected with TMPRSS2. The opposite effect was observed for chloroquine, which reduced its inhibitory activity on TMPRSS2 transfected cells (**Fig. 1E**). Our results highlight that alternative routes govern SARS-CoV-2 viral entry and these pathways vary depending on the cellular target. Thus, effective treatments may need to block both plasma membrane fusion and endosomal routes to fully achieve viral suppression.

2. Antiviral activity of compounds that potentially inhibit post-entry steps.

In our search for antivirals inhibiting post-viral entry steps, we first focused on remdesivir, which has *in vitro* activity against SARS-CoV-2 after viral entry [17] and has already been approved for the treatment of COVID-19 by the FDA and EMA. We further confirmed the *in vitro* capacity of remdesivir to inhibit SARS-CoV-2-induced cytopathic effect on Vero E6 (**Fig. 2A**). The IC_{50} value of this drug in repeated experiments was always below 10 µM (**Supp. Table 2**). In combination with increasing concentrations of hydroxychloroquine, however, remdesivir did not significantly modified its own antiviral effect (**Fig. 2B**). This was also the case for other antivirals

tested in combination (**Supp. Table 2**). Of note, other RNA polymerase inhibitors such as galdesivir, which was proposed to tightly bind to SARS-CoV-2 RNA-dependent RNA polymerase [38], showed no antiviral effect (**Supp. Table 3**). Favipiravir, approved by the National Medical Products Administration of China as the first anti-COVID-19 drug in China [39], showed only partial inhibitory activity at the non-toxic concentration of 100 µM (**Supp. Table 3**).

We also assessed clinically approved protease inhibitors with potent activity against HIV-1. However, none of the HIV-1 protease inhibitors detailed in **Supp. Table 3** showed remarkable protective antiviral activity against SARS-CoV-2 infection on Vero E6 cells, with the exception of nelfinavir mesylate hydrate, which showed an IC_{50} value below 10 µM (**Supp. Table 3** and **Fig. 2C**). Lopinavir and tipranavir inhibited SARS-CoV-2-induced cytopathic effect at the non-toxic concentration of 20 µM, and amprenavir exhibited activity at the non-toxic concentration of 100 µM (**Fig. 2C**). Darunavir, which has been tested in clinical trials, showed partial inhibitory activity at 100 µM, although this concentration had 8.5 ± 6.2 % of cytotoxicity associated (**Fig. 2C**). Of note, we tested HIV-1 reverse transcriptase inhibitors such as tenofovir disoproxil fumarate, emtricitabin, tenofovir alafenamide, and their combinations, but they also failed to show any antiviral effect against SARS-CoV-2 (**Supp. Fig. 1**). These results indicate that future clinical trials should contemplate the limited antiviral effect displayed by these anti-HIV-1 inhibitors against SARS-CoV-2 *in vitro*.

We also assessed the inhibitory capacity of HCV inhibitors, but none showed any antiviral activity (**Supp. Table 3**). Of note, exogenous interferons 2 alpha and gamma displayed antiviral activity against SARS-CoV-2 (**Supp. Table 3**). In light of these results, we tested the inhibitory effect of the TLR 7 agonist vesatolimod that triggers interferon production. Although this agonist was not able to protect from the viral-induced cytopathic effect on Vero E6 (**Supp. Table 3**), as expected since it is an interferon-producer deficient cell line [40], it could still be useful in other competent cellular targets. Since severe COVID-19 patients display impaired interferon responses [41], these strategies may be valuable to avoid disease complication. In addition, we also assessed several compounds with the best computational docking scores among approved drugs against the 3CL protease of SARS-CoV-2, but none of them were effective to protect Vero E6 from viral induced cytopathic effect (**Supp. Table 4**).

The most potent antiviral tested was plitidepsin (**Fig. 2D**), which targets the eukaryotic Elongation Factor 1A2 (eEF1A2) and has been previously used for the treatment of multiple myeloma. The mean IC_{50} value of this drug in repeated experiments was always in nM concentrations (**Supp. Table 3**). In combination with other active antivirals, we did not observe a reduction on IC_{50} values (**Supp. Table 2**). This result indicates no significant synergy, but also highlights the possibility of using plitidepsin without reducing its antiviral activity in combined therapies (**Fig. 2D**), what could be relevant to avoid possible selection of resistant viruses. Overall, plitidepsin showed the lowest IC_{50} values of all the compounds tested in this *in vitro* screening (**Table 1**).

3. Antiviral activity of compounds with unknown mechanism of action.

We also assessed the inhibitory capacity of several inhibitors and broad anti-bacterial, anti-parasitic, anti-malarial, anti-influenza and anti-fungal compounds, along with other pharmacological agents previously suggested to interfere with SARS-CoV-2 infection (**Supp. Table 5**). Such was the case of ivermectin, an FDA-approved broad spectrum anti-parasitic agent previously reported to inhibit the replication of SARS-CoV-2 *in vitro* as measured by RNA accumulation [42].

However, among these potential antivirals, only three types of molecules exerted detectable antiviral activity in our assay: itraconazole, fenofibrate, and calpain and cathepsin inhibitors such as MDL 28170 and NPO compounds. Itraconazole, an antifungal that may interfere with internal SARS-CoV-2 budding within infected cells [43], displayed an IC_{50} value of 80 µM (**Fig. 3A** and **Supp. Table 5**). Fenofibrate is clinically used to treat dyslipidemia via activation of PPARα, and also inhibited the cytopathic effect exerted by SARS-CoV-2 on Vero E6 at 20 µM (**Fig. 3B** and **Supp. Table 5**). As fenofibrate is a regulator of cellular lipid metabolism, we made use of the luciferase-based viral entry assay to try to elucidate its mode of action. When lentiviruses pseudotyped with the spike protein of SARS-CoV-2 were added to ACE2-expressing HEK-293T cells in the presence of fenofibrate, viral entry was abrogated (**Fig. 3C**). The most potent agent found was MDL 28170, a calpain III inhibitor in a pre-clinical stage of development that displayed activity in the nanomolar range (**Fig. 3D** and **Supp. Table 5**), as previously identified *in vitro* [44]. Moreover, three out of four different calpain and cathepsin inhibitors named NPO showed potent antiviral activity

too (**Supp. Figure 2**). Of note, in combination with other active antivirals, we did not observe a reduction on IC_{50} values of MDL 28170 (**Supp. Table 2**).

Inhibitors of calpains, which are cysteine proteases, might impair the activity of viral proteases like 3CL (main protease) and PLpro (papain-like protease) [44,45]. However, calpain inhibitors may also inhibit cathepsin B-mediated processing of viral spike proteins or glycoproteins, including SARS-CoV and Ebola [45,46]. To understand the mechanisms of action of calpain and cathepsin inhibitors such as MDL 28170, we added lentiviruses pseudotyped with the spike protein of SARS-CoV-2 to ACE2-expressing HEK-293T cells and the same cells also expressing TMPRSS2 in the presence of this drug. Importantly, MDL 28170 only blocked viral entry in ACE2-expressing cells (**Fig. 3E**). This result indicates that MDL 28170 blocks cathepsins that are implicated in SARS-CoV-2 entry via the alternative endosomal pathway, as described for chloroquine derivatives and E-64d (**Fig. 3E**), which are all active when TMPRSS2 is not present and their inhibitor camostat displays no activity (**Fig. 3E**).

In conclusion, among the 72 compounds and their 28 combinations tested herein for their potential capacity to abrogate SARS-CoV-2 cytopathic effect, we only found 13 compounds with antiviral activity including camostat, and only eight types of these drugs had an IC_{50} below 25 µM or 10^2 IU/mL (**Table 1**). These eight families of compounds were able to abrogate SARS-CoV-2 release to the supernatant in a dose dependent manner (**Fig. 4**), indicating that the reduction in the cytopathic effect that we had measured in cells correlates with viral production. As these eight families of compounds tackle different steps of the viral life cycle, they could be tested in combined therapies to abrogate the potential emergence of resistant viruses.

DISCUSSION

We have assessed the anti-SARS-CoV-2 activity of clinically approved compounds that may exert antiviral effect alone or in combination. Although we were not able to detect any remarkable synergy *in vitro*, combined therapies are key to tackle viral infections and to reduce the appearance of viral resistance. We have tested more than seventy compounds and their combinations, and verified a potent antiviral effect of hydroxychloroquine and remdesivir, along with plitidepsin, cathepsin and calpain inhibitors MDL 28170 and NPO, nelfinavir mesylate hydrate, interferon 2α, interferon-γ and fenofibrate. These are therefore the most promising agents found herein that were able to protect cells from viral-induced cytopathic effect by preventing viral replication.

Our findings highlight the utility of using hydroxychloroquine and MDL 28170 or other cathepsin inhibitors to block viral entry via the endosomal pathway in kidney cell lines such as Vero E6 or HEK-293T. However, the endosomal viral entry route is absent in pulmonary cells[18] and, therefore, camostat should be considered as the primary inhibitor to limit SARS-CoV-2 entry in pulmonary tissues or in cells expressing TMPRSS2[6]. These findings can explain why randomized clinical trials using hydroxychloroquine have failed to show a significant protective effect [20,21]. Nonetheless, in combined therapies, it should be noted that agents targeting the alternative endosomal SARS-CoV-2 entry route such as hydroxychloroquine or MDL 28170 could be key to stop viral dissemination in other extrapulmonary tissues where viral replication has been already detected [47], and viral entry could take place through this endosomal pathway. This could partially explain why in a retrospective observational study including more than 2500 patients, hydroxychloroquine treatment showed a significant reduction of in-hospital mortality [48]. Thus, since alternative routes govern SARS-CoV-2 viral entry depending on the cellular target [49], effective treatments might be needed to block both plasma membrane fusion and endosomal entry to broadly achieve viral suppression.

SARS-CoV-2 replication could be effectively blocked using nelfinavir mesylate hydrate, remdesivir and plitidepsin. While nelfinavir showed lower potency, remdesivir and plitidepsin were the most potent agents identified. However, remdesivir and plitidepsin are not yet suitable for oral delivery and require intravenous injection, complicating their clinical use for prophylaxis. Finally, we also confirmed the antiviral

effect of type I and II interferons as well as fenofibrate, which have been extensively used in the clinic for many years and may therefore prove valuable for therapeutic use.

The data presented herein should be interpreted with caution, as the IC_{50} values of drugs obtained *in vitro* may not reflect what could happen *in vivo* upon SARS-CoV-2 infection. The best antiviral compounds found in the present study need to be tested in adequate animal models. This strategy already helped to confirm the activity of remdesivir against SARS-CoV-2 [50], while also questioning the use of hydroxychloroquine in monotherapy [18]. Thus, assessing antiviral activity and safety in animal models is key to identify and advance those compounds with the highest potential to succeed in upcoming clinical trials. In turn, *in vitro* results confirmed in animal models will provide a rational basis to perform future clinical trials not only for treatment of SARS-CoV-2-infected individuals, but also for pre-exposure prophylaxis strategies that could avoid novel infections. Prophylaxis could be envisioned at a population level or to protect the most vulnerable groups, and should be implemented until an effective vaccine is developed. In particular, orally available compounds with proven safety profiles, such as fenofibrate, could represent promising agents.

ACKNOWLEDGEMENTS

We are grateful to patients at the Hospital Germans Trias i Pujol that donated their samples for research. For his excellent assistance and advice, we thank Jordi Puig from Fundació Lluita contra la SIDA. We are most grateful to Lidia Ruiz and the Clinical Sample Management Team of IrsiCaixa for their outstanding sample processing and management, and to M. Pilar Armengol and the translational genomics platform team at the Institut de Recerca Germans Trias i Pujol. We truly thank B. Trinité for generating the Spike expression plasmid construct used in this study. We thank Pharma Mar, Rubió Laboratories, Janssen and Drs. Cabrera and Ballana form IrsiCaixa; Pascual-Figal, Lax and Asensio-Lopez MC from "Instituto de Investigación Biosanitaria IMIB-Arrixaca" of Murcia; and Fernández-Real and Barretina from the "Institut d'Investigació Biomèdica de Girona Dr. Josep Trueta" for providing some of the reagents tested.

FINANCIAL SUPPORT

The research of CBIG consortium (constituted by IRTA-CReSA, BSC, & IrsiCaixa) is supported by Grifols pharmaceutical. The authors also acknowledge the crowdfunding initiative #Yomecorono (https://www.yomecorono.com). JS, JVA and NIU have non-restrictive funding from Pharma Mar to study the antiviral effect of plitidepsin. The funders had no role in study design, data collection and analysis, decision to publish, or preparation of the manuscript.

COMPETING INTEREST

A patent application based on this work has been filed (EP20382821.5). The authors declare that no other competing financial interests exist.

REFERENCES

1 Chen N, Zhou M, Dong X *et al.* Epidemiological and clinical characteristics of 99 cases of 2019 novel coronavirus pneumonia in Wuhan, China: a descriptive study. *The Lancet* 2020; : S0140673620302117.

2 Beigel JH, Tomashek KM, Dodd LE *et al.* Remdesivir for the Treatment of Covid-19 — Preliminary Report. *N Engl J Med* 2020; : NEJMoa2007764.

3 Grein J, Ohmagari N, Shin D *et al.* Compassionate Use of Remdesivir for Patients with Severe Covid-19. *N Engl J Med* 2020; : NEJMoa2007016.

4 WHO. "Solidarity" clinical trial for COVID-19 treatments. 2020.https://www.who.int/emergencies/diseases/novel-coronavirus-2019/global-research-on-novel-coronavirus-2019-ncov/solidarity-clinical-trial-for-covid-19-treatments (accessed 18 Aug2020).

5 Pan H. Repurposed antiviral drugs for COVID-19 –interim WHO SOLIDARITY trial results. *BioRxiv* 2020; : 17.

6 Hoffmann M, Kleine-Weber H, Krueger N, Mueller MA, Drosten C, Poehlmann S. The novel coronavirus 2019 (2019-nCoV) uses the SARS-coronavirus receptor ACE2 and the cellular protease TMPRSS2 for entry into target cells. Molecular Biology, 2020 doi:10.1101/2020.01.31.929042.

7 Monteil V, Kwon H, Prado P *et al.* Inhibition of SARS-CoV-2 infections in engineered human tissues using clinical-grade soluble human ACE2. ; : 29.

8 Mingo RM, Simmons JA, Shoemaker CJ *et al.* Ebola Virus and Severe Acute Respiratory Syndrome Coronavirus Display Late Cell Entry Kinetics: Evidence that Transport to NPC1 $^{+}$ Endolysosomes Is a Rate-Defining Step. *J Virol* 2015; **89**: 2931–2943.

9 Simmons G, Gosalia DN, Rennekamp AJ, Reeves JD, Diamond SL, Bates P. Inhibitors of cathepsin L prevent severe acute respiratory syndrome coronavirus entry. *Proc Natl Acad Sci* 2005; **102**: 11876–11881.

10 Song Z, Xu Y, Bao L *et al.* From SARS to MERS, Thrusting Coronaviruses into the Spotlight. *Viruses* 2019; **11**: 59.

11 Corman VM, Landt O, Kaiser M *et al.* Detection of 2019 novel coronavirus (2019-nCoV) by real-time RT-PCR. *Eurosurveillance* 2020; **25**. doi:10.2807/1560-7917.ES.2020.25.3.2000045.

12 Martin M. Cutadapt Removes Adapter Sequences from High-Throughput Sequencing Reads. *EMBnet.journal* 2011; **17**: 310.

13 Langmead, B., Salzberg, S. Fast gapped-read alignment with Bowtie 2. *Nat Methods* 2012; **9**: 357–359.

14 Li H, Handsaker B, Wysoker A *et al.* The Sequence Alignment/Map format and SAMtools. *Bioinformatics* 2009; **25**: 2078–2079.

15 Ou X, Liu Y, Lei X *et al.* Characterization of spike glycoprotein of SARS-CoV-2 on virus entry and its immune cross-reactivity with SARS-CoV. *Nat Commun* 2020; **11**: 1620.

16 Liu J, Cao R, Xu M *et al.* Hydroxychloroquine, a less toxic derivative of chloroquine, is effective in inhibiting SARS-CoV-2 infection in vitro. *Cell Discov* 2020; **6**: 16.

17 Wang M, Cao R, Zhang L *et al.* Remdesivir and chloroquine effectively inhibit the recently emerged novel coronavirus (2019-nCoV) in vitro. *Cell Res* 2020; **30**: 269–271.

18 Maisonnasse P, Guedj J, Contreras V *et al.* Hydroxychloroquine use against SARS-

CoV-2 infection in non-human primates. *Nature* 2020. doi:10.1038/s41586-020-2558-4.

19 Rosenke K, Jarvis MA, Feldmann F *et al*. Hydroxychloroquine Proves Ineffective in Hamsters and Macaques Infected with SARS-CoV-2. Pharmacology and Toxicology, 2020 doi:10.1101/2020.06.10.145144.

20 Boulware DR, Pullen MF, Bangdiwala AS *et al*. A Randomized Trial of Hydroxychloroquine as Postexposure Prophylaxis for Covid-19. *N Engl J Med* 2020; : NEJMoa2016638.

21 Cavalcanti AB, Zampieri FG, Rosa RG *et al*. Hydroxychloroquine with or without Azithromycin in Mild-to-Moderate Covid-19. *N Engl J Med* 2020; : NEJMoa2019014.

22 Gautret P, Lagier J-C, Parola P *et al*. Hydroxychloroquine and azithromycin as a treatment of COVID-19: results of an open-label non-randomized clinical trial. *Int J Antimicrob Agents* 2020; : 105949.

23 Gielen V, Johnston SL, Edwards MR. Azithromycin induces anti-viral responses in bronchial epithelial cells. *Eur Respir J* 2010; **36**: 646–654.

24 Hu TY, Frieman M, Wolfram J. Insights from nanomedicine into chloroquine efficacy against COVID-19. *Nat Nanotechnol* 2020. doi:10.1038/s41565-020-0674-9.

25 Phonphok Y, Rosenthal KS. Stabilization of clathrin coated vesicles by amantadine, tromantadine and other hydrophobic amines. *FEBS Lett* 1991; **281**: 188–190.

26 Wang LH, Rothberg KG, Anderson RG. Mis-assembly of clathrin lattices on endosomes reveals a regulatory switch for coated pit formation. *J Cell Biol* 1993; **123**: 1107–1117.

27 Hoffmann M. SARS-CoV-2 Cell Entry Depends on ACE2 and TMPRSS2 and Is Blocked by a Clinically Proven Protease Inhibitor. ; : 19.

28 Fantini J, Di Scala C, Chahinian H, Yahi N. Structural and molecular modelling studies reveal a new mechanism of action of chloroquine and hydroxychloroquine against SARS-CoV-2 infection. *Int J Antimicrob Agents* 2020; : 105960.

29 Lu Y, Liu DX, Tam JP. Lipid rafts are involved in SARS-CoV entry into Vero E6 cells. *Biochem Biophys Res Commun* 2008; **369**: 344–349.

30 Gassen NC, Papies J, Bajaj T *et al*. Analysis of SARS-CoV-2-controlled autophagy reveals spermidine, MK-2206, and niclosamide as putative antiviral therapeutics. Microbiology, 2020 doi:10.1101/2020.04.15.997254.

31 Jeon S, Ko M, Lee J *et al.* Identification of antiviral drug candidates against SARS-CoV-2 from FDA-approved drugs. Microbiology, 2020 doi:10.1101/2020.03.20.999730.

32 Haviernik J, Štefánik M, Fojtíková M *et al.* Arbidol (Umifenovir): A Broad-Spectrum Antiviral Drug That Inhibits Medically Important Arthropod-Borne Flaviviruses. *Viruses* 2018; **10**: 184.

33 Li. An exploratory randomized controlled study on the efficacy and safety of lopinavir/ritonavir or arbidol treating adult patients hospitalized with mild/moderate COVID-19 (ELACOI). *MedRxiv* 2020; : 33.

34 Richardson P, Griffin I, Tucker C *et al*. Baricitinib as potential treatment for 2019-nCoV acute respiratory disease. *The Lancet* 2020; **395**: e30–e31.

35 Stebbing J, Phelan A, Griffin I *et al.* COVID-19: combining antiviral and anti-inflammatory treatments. *Lancet Infect Dis* 2020; **20**: 400–402.

36 Münch J. Alpha-1 antitrypsin inhibits SARS-CoV-2 infection. *BioRxiv* 2020; : 14.

37 Oguntuyo. In plain sight: the role of alpha-1-antitrypsin in COVID-19 pathogenesis and therapeutics. *BioRxiv* 2020. doi:doi: 10.1101/2020.08.14.248880.

38 Elfiky AA. Ribavirin, Remdesivir, Sofosbuvir, Galidesivir, and Tenofovir against SARS-CoV-2 RNA dependent RNA polymerase (RdRp): A molecular docking study. *Life Sci* 2020; **253**: 117592.
39 Tu Y-F, Chien C-S, Yarmishyn AA *et al.* A Review of SARS-CoV-2 and the Ongoing Clinical Trials. *Int J Mol Sci* 2020; **21**: 2657.
40 Emeny JM, Morgan MJ. Regulation of the Interferon System: Evidence that Vero Cells have a Genetic Defect in Interferon Production. *J Gen Virol* 1979; **43**: 247–252.
41 Hadjadj J, Yatim N, Barnabei L *et al.* Impaired type I interferon activity and inflammatory responses in severe COVID-19 patients. *Science* 2020; : eabc6027.
42 Caly L, Druce JD, Catton MG, Jans DA, Wagstaff KM. The FDA-approved Drug Ivermectin inhibits the replication of SARS-CoV-2 in vitro. *Antiviral Res* 2020; : 104787.
43 Wu C, Liu Y, Yang Y *et al.* Analysis of therapeutic targets for SARS-CoV-2 and discovery of potential drugs by computational methods. *Acta Pharm Sin B* 2020; **10**: 766–788.
44 Riva L, Yuan S, Yin X *et al.* Discovery of SARS-CoV-2 antiviral drugs through large-scale compound repurposing. *Nature* 2020. doi:10.1038/s41586-020-2577-1.
45 Schneider M, Ackermann K, Stuart M *et al.* Severe Acute Respiratory Syndrome Coronavirus Replication Is Severely Impaired by MG132 due to Proteasome-Independent Inhibition of M-Calpain. *J Virol* 2012; **86**: 10112–10122.
46 Zhou Y, Simmons G. Development of novel entry inhibitors targeting emerging viruses. *Expert Rev Anti Infect Ther* 2012; **10**: 1129–1138.
47 Hanley B, Naresh KN, Roufosse C *et al.* Histopathological findings and viral tropism in UK patients with severe fatal COVID-19: a post-mortem study. *Lancet Microbe* 2020; : S2666524720301154.
48 Arshad S, Kilgore P, Chaudhry ZS *et al.* Treatment with hydroxychloroquine, azithromycin, and combination in patients hospitalized with COVID-19. *Int J Infect Dis* 2020; **97**: 396–403.
49 Ou T, Mou H, Zhang L, Ojha A, Choe H, Farzan M. Hydroxychloroquine-mediated inhibition of SARS-CoV-2 entry is attenuated by TMPRSS2. Microbiology, 2020 doi:10.1101/2020.07.22.216150.
50 Williamson B, Feldmann F, Schwarz B *et al.* Clinical benefit of remdesivir in rhesus macaques infected with SARS-CoV-2. Microbiology, 2020 doi:10.1101/2020.04.15.043166.

TABLES

Table 1. Compounds with antiviral activity grouped in colors depending on their IC_{50} values on Vero E6. Green color highlights compounds with the lower IC_{50} in the nM range, while orange color shows compounds in the µM or 10^2 IU/mL range.

FIGURES

Figure 1. Antiviral activity of entry inhibitors against SARS-CoV-2. **A.** Antiviral activity of hydroxychloroquine and azithromycin. Cytopathic effect on Vero E6 cells exposed to a fixed concentration of SARS-CoV-2 in the presence of increasing concentrations of hydroxychloroquine, azithromycin, and their combination. Drugs were used at a concentration ranging from 0.0512 nM to 100 µM. When combined, each drug was added at the same concentration. Non-linear fit to a variable response curve from one representative experiment with two replicates is shown (red lines), excluding data from drug concentrations with associated toxicity. The particular IC_{50} value of this graph is indicated. Cytotoxic effect on Vero E6 cells exposed to increasing concentrations of drugs in the absence of virus is also shown (grey lines). **B.** Cytopathic effect on Vero E6 cells exposed to a fixed concentration of SARS-CoV-2 in the presence of increasing concentrations of amantadine, a clathrin-mediated endocytosis inhibitor, E-64d, a pan-cathepsin inhibitor acting downstream once viruses are internalized in endosomes, NB-DNJ, an inhibitor of ganglioside biosynthesis and methyl-β-cyclodextrin, a cholesterol-depleting agent. All drugs were used at a concentration ranging from 0.0512 nM to 100 µM aside from methyl-β-cyclodextrin, which was used 10 times more concentrated. Non-linear fit to a variable response curve from one experiment with two replicates is shown (red lines). Cytotoxic effect on Vero E6 cells exposed to increasing concentrations of drugs in the absence of virus is also shown (grey lines). **C.** Cytopathic effect on Vero E6 cells exposed to a fixed concentration of SARS-CoV-2 in the presence of increasing concentrations of camostat, a TMPRSS2 inhibitor, and ATT, an alpha-1 antyitrypsin, a broad cellular protease inhibitor, as described in **A**. **D.** Effect of entry inhibitors on luciferase expression of reporter lentiviruses pseudotyped with SARS-CoV-2 Spike in ACE2 expressing HEK-293T cells. Values are normalized to luciferase expression by mock-treated cells set at 100%. Mean and s.e.m. from two experiments with one to three replicates. Cells were exposed to fixed amounts of SARS-CoV-2 Spike lentiviruses in the presence of a non-

toxic constant concentration of the drugs tested on Vero E6. Significant statistical deviations from 100% were assessed with a one sample t test. **E.** Comparison of entry inhibitors blocking viral endocytosis, such as chloroquine, with inhibitors blocking serine protease TMPRSS2 expressed on the cellular membrane, such as camostat, on different cell lines. ACE2 expressing HEK-293T cells transfected or not with TMPRSS2 were exposed to SARS-CoV-2 Spike lentiviruses as described in **B**. Values are normalized to luciferase expression by mock-treated cells set at 100%. Mean and s.e.m. from at least two representative experiments with two replicates. Statistical deviations from 100% were assessed with a one sample t test.

Figure 2. Antiviral activity of post-entry inhibitors. **A.** Cytopathic effect on Vero E6 cells exposed to a fixed concentration of SARS-CoV-2 in the presence of increasing concentrations of Remdesivir. Drug was used at a concentration ranging from 0.0512 nM to 100 µM. Non-linear fit to a variable response curve from one representative experiment with two replicates is shown (red lines), excluding data from drug concentrations with associated toxicity. The particular IC_{50} value of this graph is indicated. Cytotoxic effect on Vero E6 cells exposed to increasing concentrations of drugs in the absence of virus is also shown (grey lines). **B.** Cytopathic effect on Vero E6 cells exposed to a fixed concentration of SARS-CoV-2 in the presence of increasing concentrations of remdesivir and its combination with hydroxychloroquine, as detailed in **A**. Drugs in combination were used at a concentration ranging from 0.0512 nM to 100 µM (left panel). **C.** Cytopathic effect on Vero E6 cells exposed to a fixed concentration of SARS-CoV-2 in the presence of increasing concentrations of protease inhibitors against HIV-1. Nelfinavir mesylate hydrate was the only drug with activity. Inhibitors were used at a concentration ranging from 0.0512 nM to 100 µM. The particular IC_{50} value of this graph is indicated **D.** Cytopathic effect on Vero E6 cells exposed to a fixed concentration of SARS-CoV-2 in the presence of increasing concentrations of plitidepsin and its combinations with hydroxychloroquine and remdesivir. When combined, each drug was added at the same concentration. Drugs were used at a concentration ranging from 0.5 nM to 10 µM. The particular IC_{50} value of these graphs is indicated.

Figure 3. Antiviral activity of inhibitors with unknown mechanism of action. **A.** Cytopathic effect on Vero E6 cells exposed to a fixed concentration of SARS-CoV-2 in

the presence of increasing concentrations of Itraconazole. Drug was used at a concentration ranging from 0.0512 nM to 100 µM . Non-linear fit to a variable response curve from one representative experiment with two replicates is shown (red lines), excluding data from drug concentrations with associated toxicity. The particular IC_{50} value of this graph is indicated. Cytotoxic effect on Vero E6 cells exposed to increasing concentrations of drugs in the absence of virus is also shown (grey lines). **B.** Cytopathic effect on Vero E6 cells exposed to a fixed concentration of SARS-CoV-2 in the presence of increasing concentrations of Fenofibrate, as detailed in **A**. **C**. Effect of fenofibrate on the entry of luciferase expressing lentiviruses pseudotyped with SARS-CoV-2 Spike in ACE2-expressing HEK-293T cells. Values are normalized to luciferase expression by mock-treated cells set at 100%. Mean and s.e.m. from two experiments with two replicates. Statistical deviations from 100% were assessed with a one sample t test. **D**. Cytopathic effect on Vero E6 cells exposed to a fixed concentration of SARS-CoV-2 in the presence of increasing concentrations of MDL 28170, as detailed in **A**. **E**. Comparison of MDL 28170 activity with entry inhibitors blocking viral endocytosis, such as chloroquine and E-64d, and inhibitors blocking serine protease TMPRSS2, such as camostat. ACE2 expressing HEK-293T cells transfected or not with TMPRSS2 were exposed to SARS-CoV-2 Spike lentiviruses in the presence of these compounds. Values are normalized to luciferase expression by mock-treated cells set at 100%. Mean and s.e.m. from at least two experiments with two replicates. Statistical deviations from 100% were assessed with a one sample t test.

Figure 4. Decreased release of SARS-CoV-2 in the presence of inhibitors with antiviral activity. **A.** Viral release to the supernatant in the presence of the indicated compounds added at increasing concentrations 3 days post-infection of Vero E6 cells. SARS-CoV-2 nucleoprotein was detected with an ELISA at concentrations were drugs were nontoxic. Mean and s.e.m. from two experiments. **B.** Viral release to the supernatant in the presence of the indicated interferons as described in A. Mean and s.e.m. from one experiment.

SUPPLEMENTARY TABLES

Supp. Table 1. Antiviral activity of potential entry inhibitors tested against SARS-CoV-2. IC_{50} values are reported in µM unless otherwise indicated. “Not active” refers to the lack of inhibitory activity at the highest concentration tested for each compound.

Supp. Table 2. List of combinations of active antivirals that did not show any enhanced antiviral activity when mixed. Synergy was defined as showing an enhanced IC_{50} in drug combination as compared to the highest IC_{50} of the most potent compound tested. Similar toxicity is reported if viability was found to be similar to the most toxic compound tested in the combination, while higher toxicity reports an increase above 10% in cytotoxicity in the combination.

Supp. Table 3. Antiviral activity of potential post-entry inhibitors against SARS-CoV-2. IC_{50} values are reported in µM unless otherwise indicated. "Not active" refers to the lack of inhibitory activity at the highest concentration tested for each compound.

Supp. Table 4. Antiviral activity of potential inhibitors against SARS-CoV-2 with predicted capacity to block SARS-CoV-2 viral protease. "Not active" refers to the lack of inhibitory activity at the highest concentration tested for each compound. All compounds but the two indicated were found non-toxic at 100 µM.

Supp. Table 5. Antiviral activity of potential inhibitors against SARS-CoV-2 with unknown mechanism of action. IC_{50} values are reported in µM. "Not active" refers to the lack of inhibitory activity at the highest concentration tested for each compound.

SUPPLEMENTARY FIGURES

Supplementary Figure 1. No antiviral activity of HIV-1 reverse transcriptase inhibitors. Cytopathic effect on Vero E6 cells exposed to a fixed concentration of SARS-CoV-2 in the presence of increasing concentrations of HIV-1 reverse transcriptase inhibitors. Drugs were used at a concentration ranging from 0.0512 nM to 100 µM. Non-linear fit to a variable response curve from one experiment with two replicates is shown (red lines). Cytotoxic effect on Vero E6 cells exposed to increasing concentrations of drugs in the absence of virus is also shown (grey lines).

Supplementary Figure 2. Antiviral activity of NPO calpain and cathepsin inhibitors. Cytopathic effect on Vero E6 cells exposed to a fixed concentration of SARS-CoV-2 in the presence of increasing concentrations of calpain and cathepsin inhibitors NPO. MDL 28170 was used at a concentration ranging from 0.0512 nM to 100 µM, while NPO was used from 0.00512 nM to 10 µM . Non-linear fit to a variable response curve from one experiment with two replicates is shown (red lines). Cytotoxic effect on Vero

E6 cells exposed to increasing concentrations of drugs in the absence of virus is also shown (grey lines).

AUTHOR CONTRIBUTION

Conceived and designed the experiments: JR, JMB, DPZ, JS, BC, JVA, NIU

Performed in silico drug modeling: VG

Performed experiments: JR, JMB, DPZ, MNJ, IE, VG, JVA, NIU

Contributed with critical reagents: CQ, IB

Analyzed and interpreted the data: JR, JMB, DPZ, MNJ, RP, LM, CQ, IE, IB, AV, VG, JC, JB, JS, BC, JVA, NIU

Wrote the paper: JR, JVA, NIU

DATA AVAILABILITY Data is available from corresponding authors upon reasonable request.

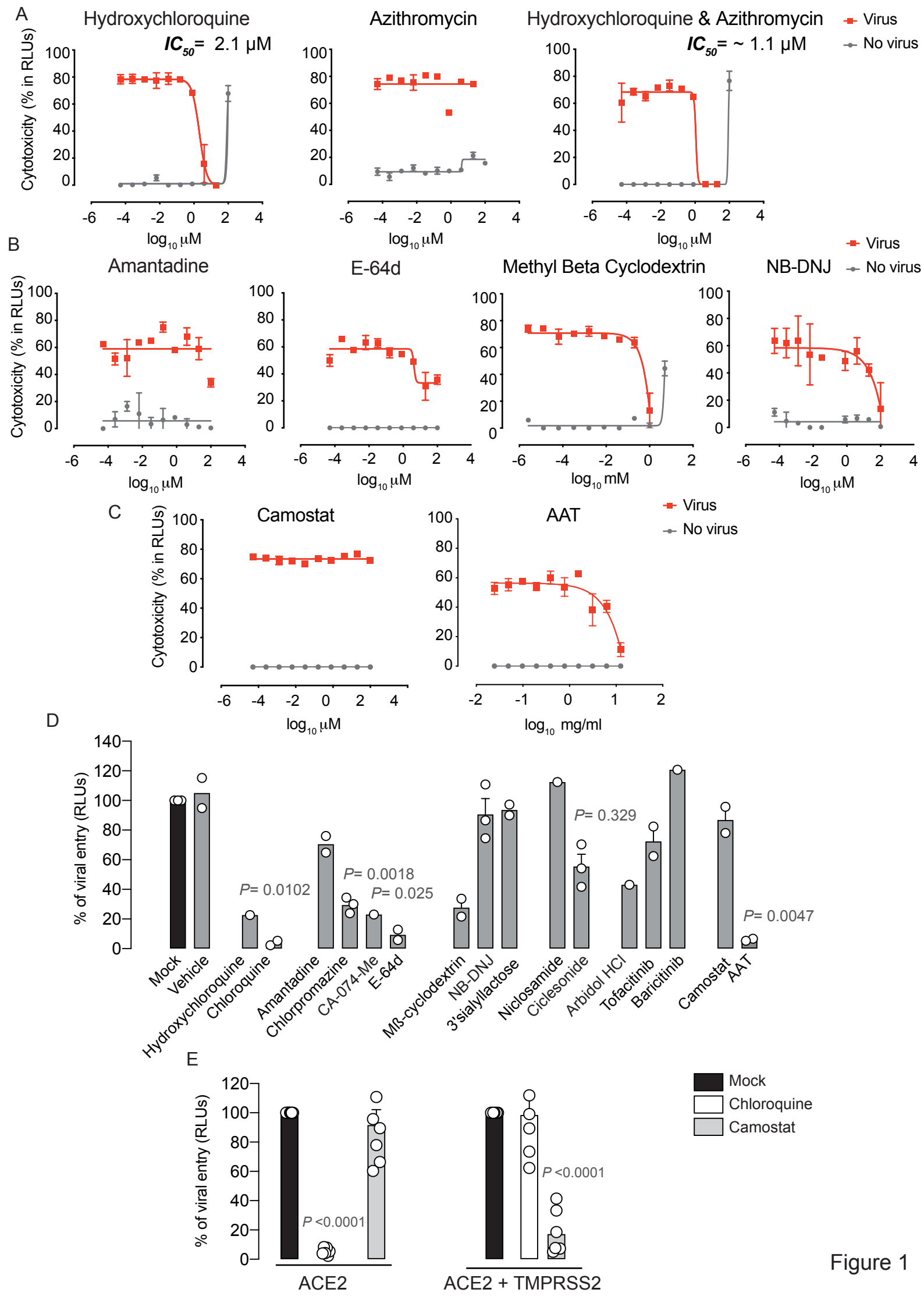
A
Hydroxychloroquine
IC50= 2.1 μM
Azithromycin
Hydroxychloroquine & Azithromycin
IC50= ~ 1.1 μM
Virus
No virus
Cytotoxicity (% in RLUs)
log10 μM
B
Amantadine
E-64d
Methyl Beta Cyclodextrin
NB-DNJ
log10 mM
C
Camostat
AAT
log10 mg/ml
D
% of viral entry (RLUs)
P= 0.0102
P= 0.0018
P= 0.025
P= 0.329
P= 0.0047
Mock
Vehicle
Hydroxychloroquine
Chloroquine
Amantadine
Chlorpromazine
CA-074-Me
E-64d
Mß-cyclodextrin
NB-DNJ
3'sialyllactose
Niclosamide
Ciclesonide
Arbidol HCl
Tofacitinib
Baricitinib
Camostat
AAT
E
Mock
Chloroquine
Camostat
P <0.0001
P <0.0001
ACE2
ACE2 + TMPRSS2

Figure 1

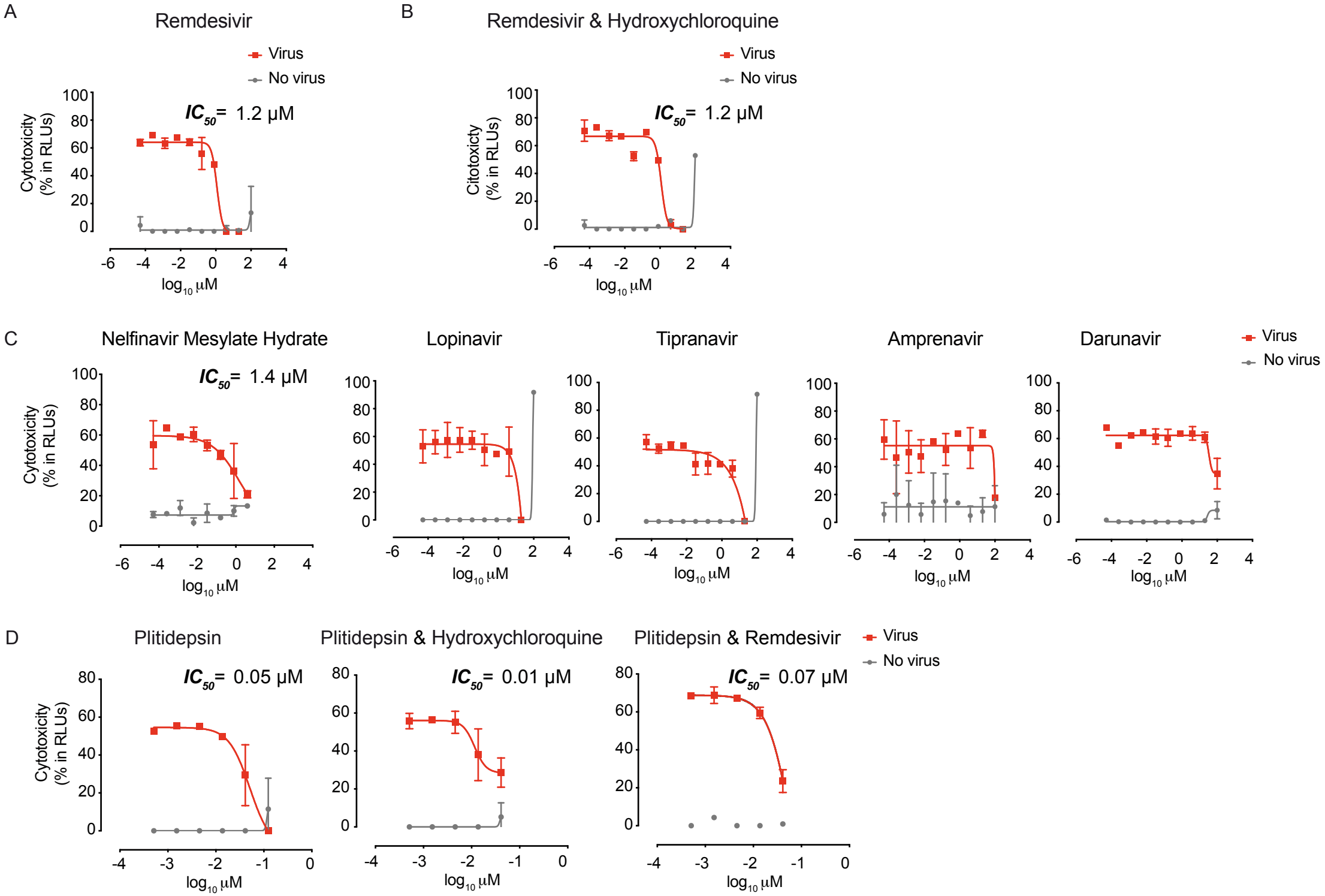
A
Remdesivir
Virus
No virus
Cytotoxicity (% in RLUs)
IC50= 1.2 μM
log10 μM
B
Remdesivir & Hydroxychloroquine
Virus
No virus
Citotoxicity (% in RLUs)
IC50= 1.2 μM
log10 μM
C
Nelfinavir Mesylate Hydrate
IC50= 1.4 μM
Lopinavir
Tipranavir
Amprenavir
Darunavir
Virus
No virus
Cytotoxicity (% in RLUs)
log10 μM
D
Plitidepsin
IC50= 0.05 μM
Plitidepsin & Hydroxychloroquine
IC50= 0.01 μM
Plitidepsin & Remdesivir
IC50= 0.07 μM
Virus
No virus
Cytotoxicity (% in RLUs)
log10 μM

Figure 2

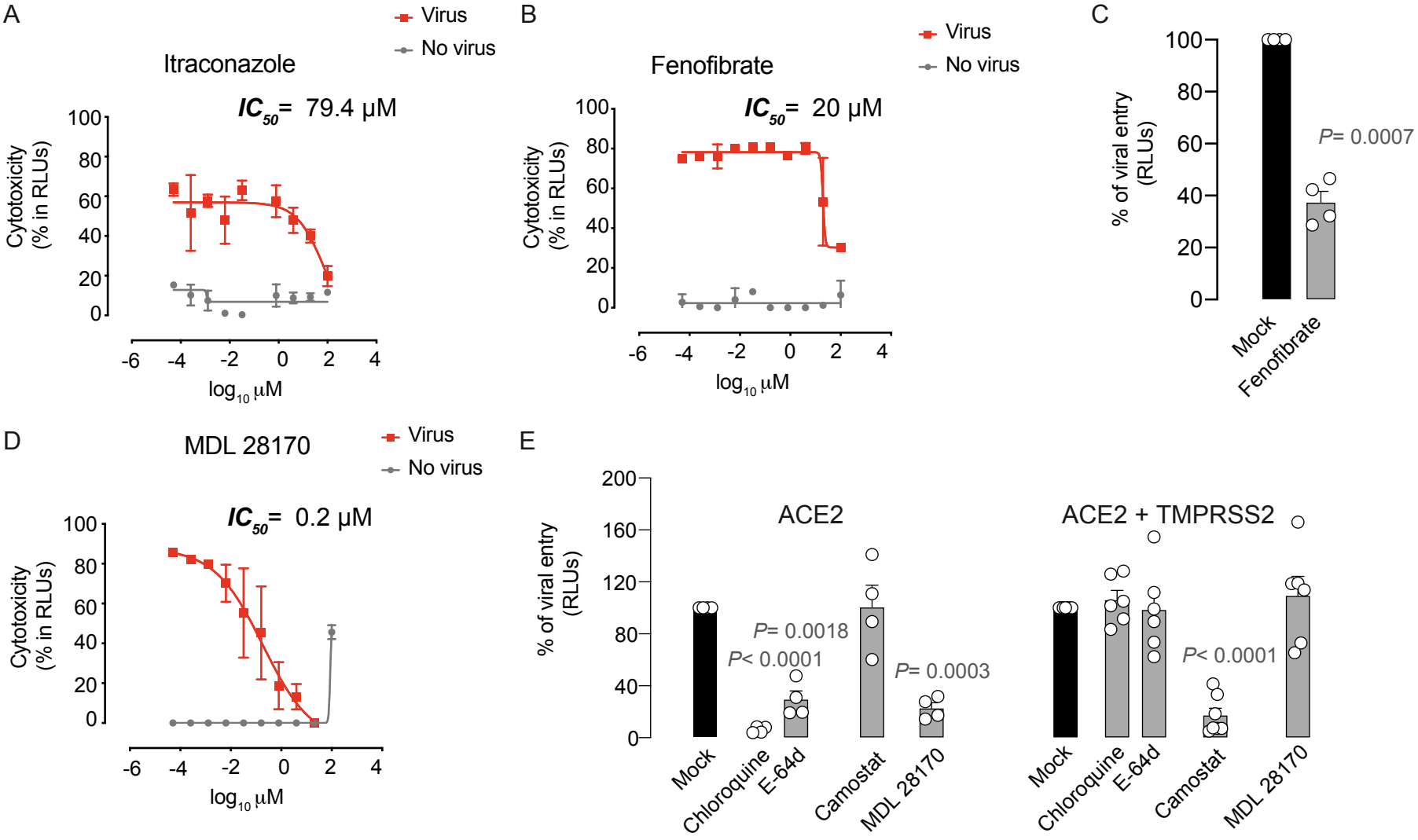
A
Virus
No virus
Itraconazole
IC50= 79.4 µM
Cytotoxicity (% in RLUs)
log10 µM
B
Virus
No virus
Fenofibrate
IC50= 20 µM
Cytotoxicity (% in RLUs)
log10 µM
C
% of viral entry (RLUs)
P= 0.0007
Mock
Fenofibrate
D
Virus
No virus
MDL 28170
IC50= 0.2 µM
Cytotoxicity (% in RLUs)
log10 µM
E
% of viral entry (RLUs)
ACE2
P= 0.0018
P< 0.0001
P= 0.0003
Mock
Chloroquine
E-64d
Camostat
MDL 28170
ACE2 + TMPRSS2
P< 0.0001
Mock
Chloroquine
E-64d
Camostat
MDL 28170

Figure 3

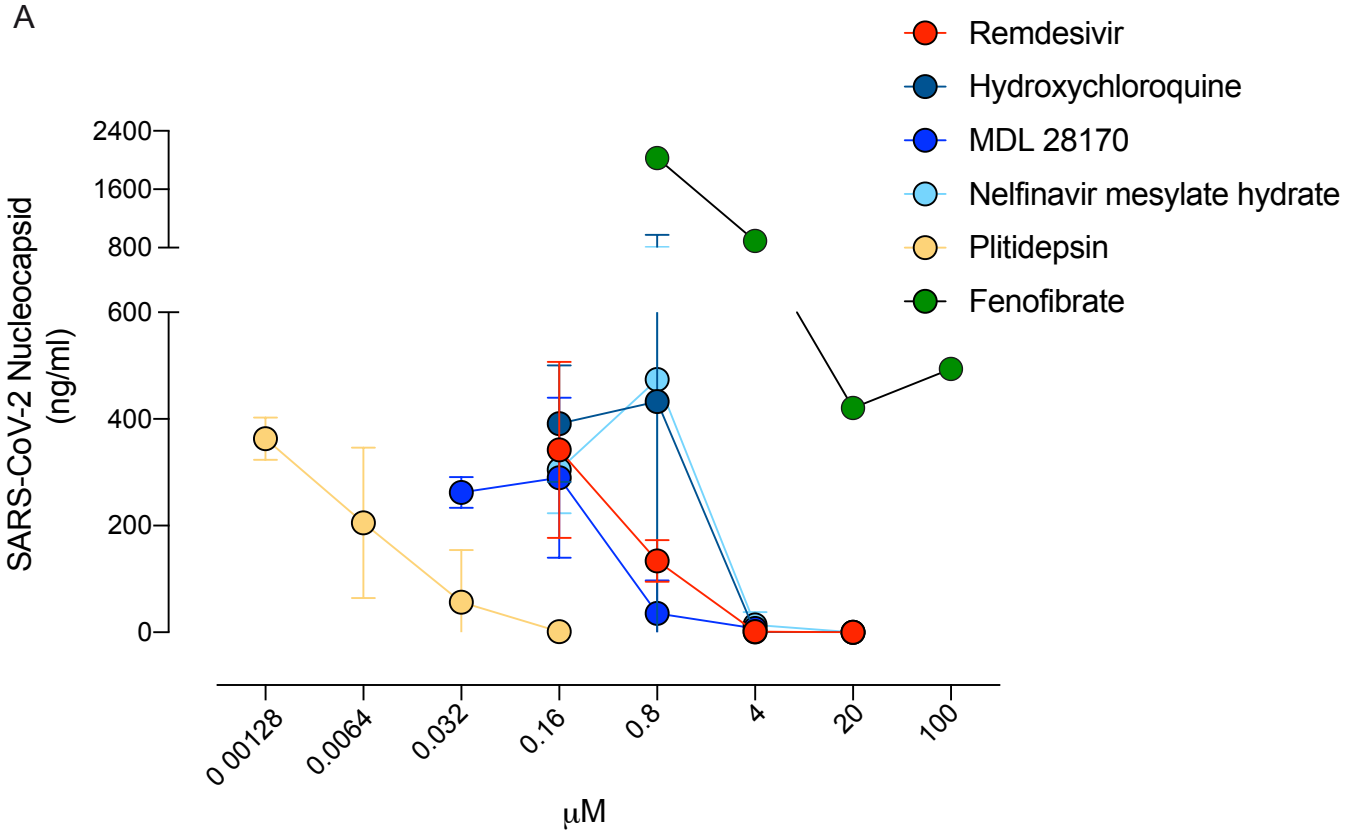
A
Remdesivir
Hydroxychloroquine
MDL 28170
Nelfinavir mesylate hydrate
Plitidepsin
Fenofibrate
SARS-CoV-2 Nucleocapsid (ng/ml)
2400
1600
800
600
400
200
0
0 00128
0.0064
0.032
0.16
0.8
4
20
100
µM

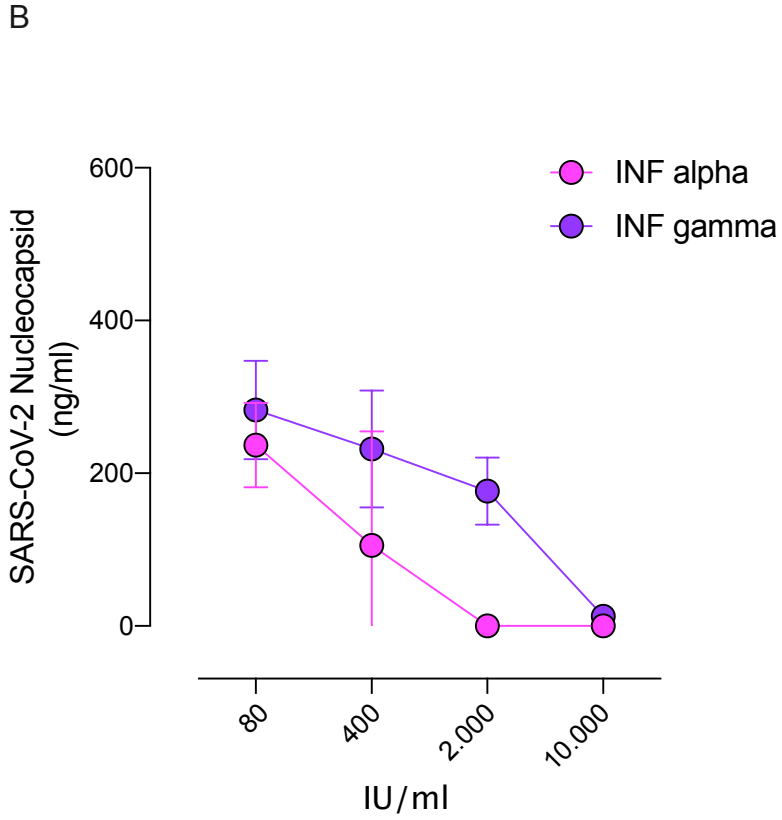
B
INF alpha
INF gamma
SARS-CoV-2 Nucleocapsid (ng/ml)
600
400
200
0
80
400
2.000
10.000
IU/ml

Figure 4

	DRUG	IC_{50} / CC_{50} µM (Mean +/-SD)	Mode of Action	Previous Clinical Use	Vendor Origen
nM	Plitidepsin	0.06 +/- 0.02 / > 0.1	Targets eukaryotic Elongation Factor 1A2 (eEF1A2)	Multiple myeloma	PharmaMar
	MDL 28170	0.14 +/- 0.06 / > 87	Calpain III inhibitor & Cathepsin B	*Pre-Clinical*	Merck
	NPO-2142; -2143 & -2260	~ 0.54 / >10	Calpain & Cathepsin inhibitors	*Pre-Clinical*	Landsteiner Genmed
< 25 µM or 10^2 IU/mL	Remdesivir	2.16 +/-4.1 / > 85	RNA Polymerase inhibitor	Ebola Virus	Cayman Chemical
	Hydroxycloroquine	10.9 +/- 11.3 / > 96	Clathrin-mediated endocitosys or pH-dependent viral fusion inhibitor	Malaria	Laboratorios Rubio
	Nelfinavir mesylate hydrate	*Not calculated, but active < 10 I* > 25	Protease inhibitor	HIV-1	Sigma Aldrich
	Chloroquine	3.86 / > 25	Clathrin-mediated endocitosys or pH-dependent viral fusion inhibitor	Malaria	Sigma Aldrich
	Interferon 2 alpha	8.1+/-0.7 $x10^2$ IU/mL / >100 $x10^2$ IU/mL	INF stimulated antiviral proteins	Hepatitis & HIV-1	Sigma-Aldrich
	Interferon gamma	11.2 $x10^2$ IU/mL / >100 $x10^2$ IU/mL	INF stimulated antiviral proteins	Granulomatous disease	Sigma-Aldrich
	Fenofibrate	19.8+/- 8 / >100	Activates PPARα	Dyslipidemia	Lacer

Table 1

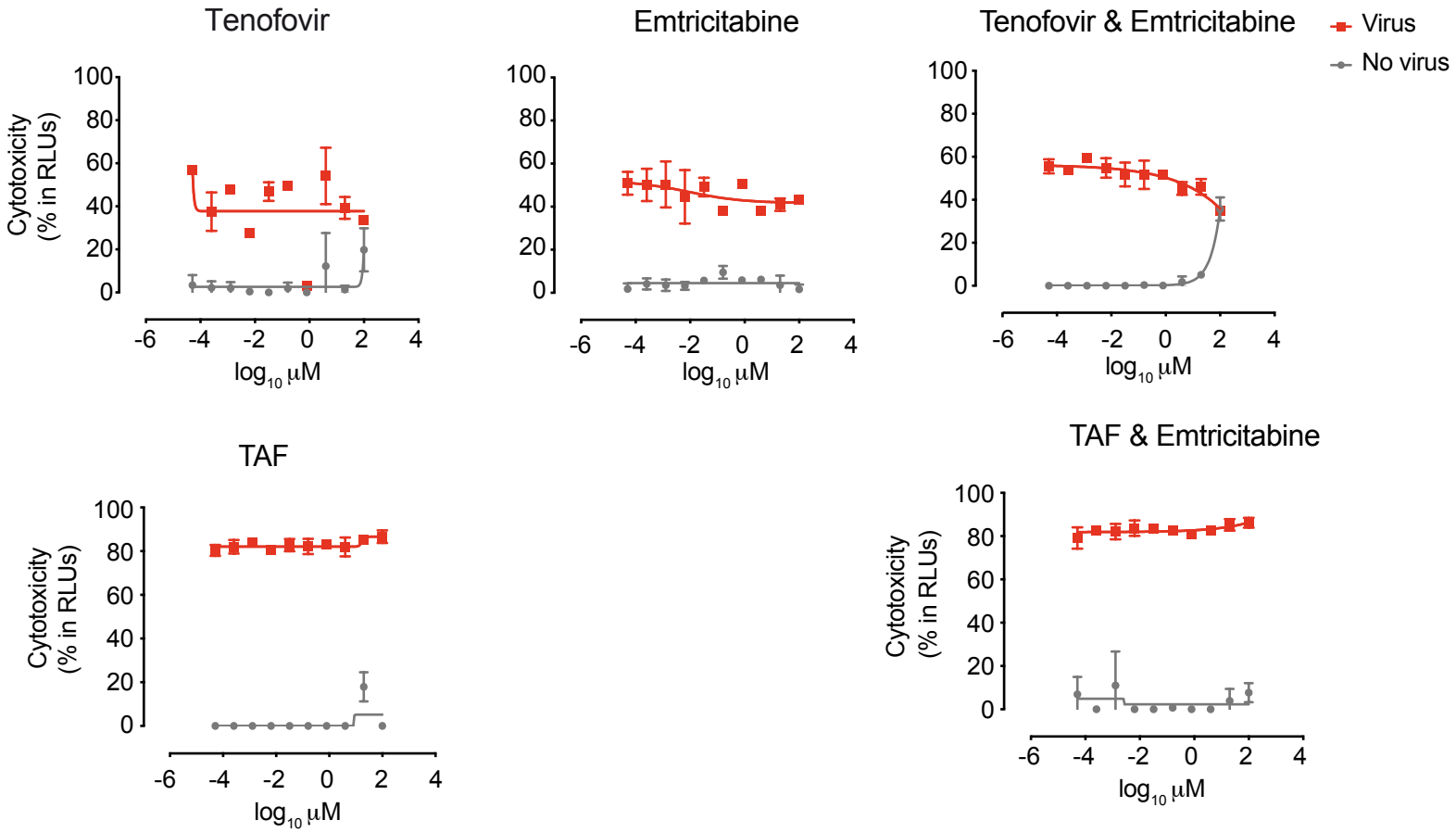

Supplementary Figure 1

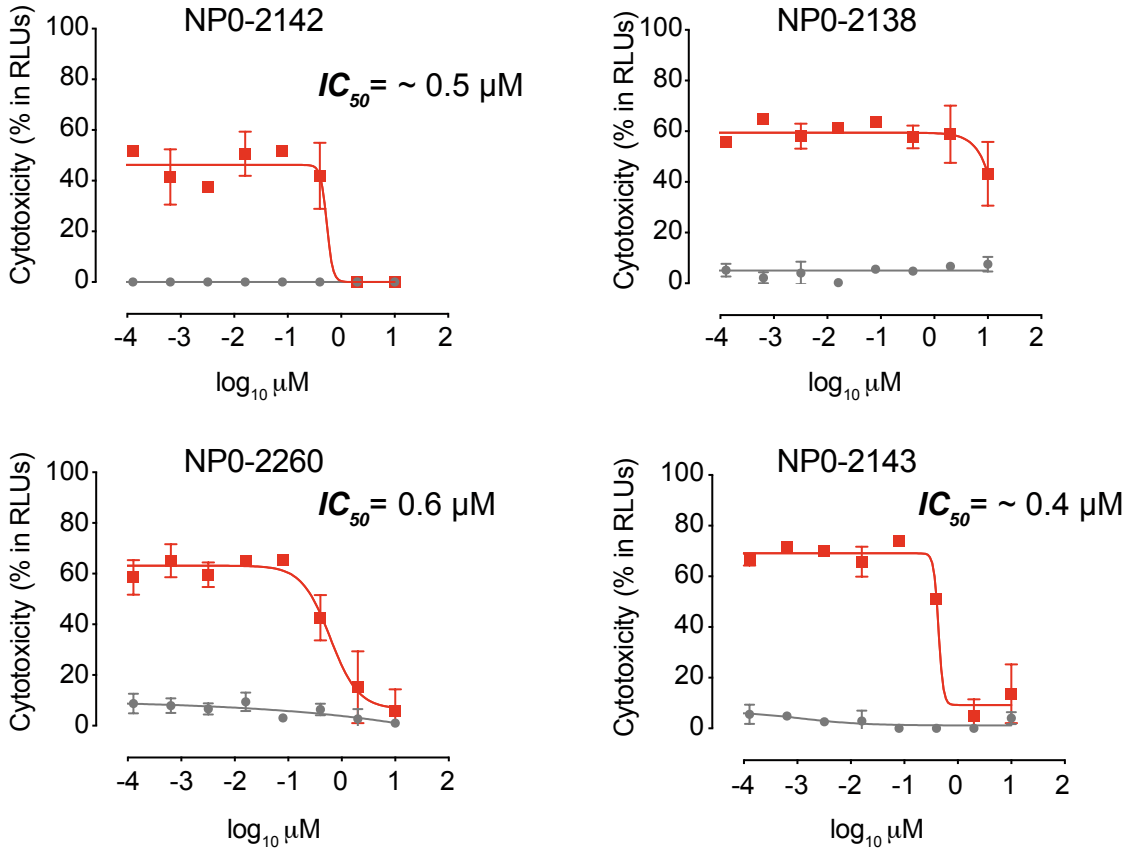

Supplementary Figure 2

ACTIVITY	DRUG	IC_{50} / CC_{50} µM (Mean +/-SD)	Mode of Action	Previous Clinical Use	Vendor Origen
ENTRY	Hydroxychloroquine	9.3 +/- 11.1 / > 80	Clathrin-mediated endocitosys or pH-dependent viral fusion inhibitor	Malaria	Laboratorios Rubió
	Chloroquine	3.9 / > 25			Sigma Aldrich
	Amantadine	*Not calculated, but partialy active at 100 /* > 100	Clathrin-mediated endocitosys inhibitor	Parkinson & influenza A	Sigma Aldrich
	Chlorpromazine (Largactil)	Not Active / > 18	Clathrin-mediated endocitosys inhibitor	Antipsychotic	Sanofi
	CA-074-Me	Not Active / > 34	Cathepsin inhibitor B	*Pre-Clinical*	Sigma Aldrich
	E-64d	*Not calculated, but partialy active at 100* / > 100	Cathepsin inhibitor B/L	*Pre-Clinical*	Sigma Aldrich
	Methyl-ß-cyclodextrin	*Not calculated, but active at 1000*	Cholesterol-removing agent, lipid raft disruption	*Not approved*	Sigma Aldrich
	NB-DNJ	*Not calculated, but active at 100* / > 100	Inhibits ceramide- glucosyltransferase and β-glucosidase 2	Gaucher disease & Juvenile Sandhoff disease	Calbiochem
	3' Sialyllactose Na Salt	Not Active / 20 mM	Inhibits viral binding	*Pre-Clinical*	Carbosynth
	Niclosamide	Not Active / > 9	Beclin-1 stabilizer in autophagy	Helmints	Selleckchem
	Ciclesonide	Not Active / > 20	Glucocorticoid	Asthma	Selleckchem
	Arbidol HCl	Not Active / > 40	Fusion inhibitor?	Influenza	Selleckchem
	Tofacitinib (Xeljanx)	Not Active / > 100	JAK inhibitor	Rheumatoid arthritis	Pfizer
	Baricitinib	Not Active / > 85	JAK inhibitor	Rheumatoid arthritis	Selleckchem
	Camostat	Not Active / > 100	TMPRSS2 inhibitor	Chronic pancreatitis	Merck
	Alpha-1 Antitrypsin	*Not calculated, but active at 12.5 mg/ml* / > 12.5 mg/ml	Cellular protease inhibitor	Alpha-1 antitrypsin deficiency	Grifols

Supplementary Table 1

DRUG 1	DRUG 2	DRUG 3	DRUG 4	Synergy	Toxicity in combination
Hydroxy-Cloroquine	Azithromycin			No	Similar
	Lopinavir			No	Similar
	Tipranavir			No	Similar
	Amprenavir			No	Similar
	Darunavir			No	Similar
	Baricitinib			No	Similar
	Tenofovir	Emtricitabine		No	Similar
	TAF	Emtricitabine		No	Similar
Remdesivir	Hydroxychloroquine			No	Similar
	Amantadine			No	Similar
	Chlorpromazine			No	Similar
	Baricitinib			No	Higher
	Tipranavir	Lopinavir		No	Similar
Lopinavir	Ritonavir			No	Higher
	Tipranavir			No	Higher
	Ritonavir	Tenofovir	Emtricitabine	No	Similar
	Ritonavir	Tenofovir Alafenamide	Emtricitabine	No	Similar
Tipranavir	Tenofovir	Emtricitabine		No	Similar
Tenofovir	Emtricitabine			No	Similar
Nelfinavir Mesylate Hydrate	Hydroxychloroquine			No	Similar
	Remdesivir			No	Similar
MDL28170	Hydroxychloroquine			No	Similar
	Remdesivir			No	Similar
	Nelfinavir Mesylate Hydrate			No	Similar
Plitidepsin	Hydroxychloroquine			No	Similar
	Remdesivir			No	Similar
	MDL 28170			No	Similar
	Nelfinavir Mesylate Hydrate			No	Similar

Supplementary Table 2

ACTIVITY	DRUG	IC_{50} / CC_{50} µM (Mean +/-SD)	Mode of Action	Previous Clinical Use	Vendor Origen
POST-ENTRY	Remdesivir	2.2 +/-4.1 / > 85	RNA Polymerase inhibitor	Ebola Virus	Cayman Chemical
	Galdesivir	Not Active / 100	RNA Polymerase inhibitor	YFV	MedChemExpress
	Favipiravir	*Not calculated, but partially active at 100* / > 100	RNA polimerase inhibitor	Flavivirus, Arenavirus, Bunyavirus, Alphavirus	Quimigen
	Saquinavir	Not Active / > 28	Protease inhibitor	HIV-1	Reference standard HPLC
	Lopinavir	*Not calculated, but active at 20* / > 87	Protease inhibitor	HIV-1	Abbot
	Ritonavir	*Not active* / 20-100	Protease inhibitor	HIV-1	Abbot
	Tipranavir	*Not calculated, but active at 20* / > 70	Protease inhibitor	HIV-1	Reference standard HPLC
	Nelfinavir Mesylate Hydrate	*Not calculated, but active <10* / > 25	Protease inhibitor	HIV-1	Sigma Aldrich
	Amprenavir	*Not calculated, but active at 100* / > 100	Protease inhibitor	HIV-1	GSK
	Fosamprenavir Calcium	Not Active / > 25	Protease inhibitor	HIV-1	Sigma Aldrich
	Darunavir	*Not calculated, but partially active at 100* / > 100	Protease inhibitor	HIV-1	Sigma Aldrich
	Atazanavir Sulfate	Not Active / > 20	Protease inhibitor	HIV-1	Reference standard HPLC
	Tenofovir disoproxil fumarate	Not Active / > 100	Reverse Transcriptase inhibitor	HIV-1	Selleckchem
	Emtricitabine (Emtriva)	Not Active / > 100	Reverse Transcriptase inhibitor	HIV-1	Gilead
	Tenofovir Alafenamide	Not Active / > 100	Reverse Transcriptase inhibitor	HIV-1	Selleckchem
	Velpatasvir	Not Active / > 10	Iinhibitor of NS5A protein	HCV	Selleckchem
	Sofosbuvir	Not Active / > 100	Polymerase inhibitor	HCV	Selleckchem
	Boceprevir	Not Active / > 100	Protease inhibitor	HCV	Quimigen
	Vesatolimod	Not Active / > 20	TLR7 agonist	Hepatitis & HIV-1	MedChemExpress
	Interferon 2 alpha	8.1+/-0.7 $x10^2$ IU/mL / >100 $x10^2$ IU/mL	IFN stimulated antiviral proteins	Hepatitis & HIV-1	Sigma-Aldrich
	Interferon gamma	11.2 $x10^2$ IU/mL / >100 $x10^2$ IU/mL	IFN stimulated antiviral proteins	Granulomatous disease	Sigma-Aldrich
	Plitidepsin	0.06 +/- 0.02 / > 0.1	Targets eukaryotic Elongation Factor 1A2 (eEF1A2)	Multiple myeloma	PharmaMar

Supplementary Table 3

Bioinformatic ANALYSIS	DRUG	IC_{50} / CC_{50} µM (Mean +/-SD)	Mode of Action	Previous Clinical Use	Vendor Origen
	Salbutamol	Not Active	Predicted SARS-Cov-2 Protease inhibitor	Asthma	Sigma Aldrich
	Diclondazolic acid (Lonidamine)	Not Active	Predicted SARS-Cov-2 Protease inhibitor	Anticancer	Abcam
	Thiocolchicoside	Not Active	Predicted SARS-Cov-2 Protease inhibitor	Skeletal muscle relaxant	Sigma Aldrich
	Morphothiadine	Not Active / 54	Predicted SARS-Cov-2 Protease inhibitor	Hepatitis B	Quimigen
	Ingliforib	Not Active	Predicted SARS-Cov-2 Protease inhibitor	Glycogen phosphorylase inhibitor	Quimigen
	Perampanel	Not Active	Predicted SARS-Cov-2 Protease inhibitor	Antiepileptic	Quimigen
	Montirelin trifluoroacetate salt	Not Active	Predicted SARS-Cov-2 Protease inhibitor	Thyrotropin-releasing hormone agonists	Sigma Aldrich
	Saquinavir	Not Active	Predicted SARS-Cov-2 Protease inhibitor	HIV-1	Reference standard HPLC
	Pamicogrel	Not Active / 6.4	Predicted SARS-Cov-2 Protease inhibitor	Antiplatelet aggregation	Quimigen
	Pomalidomide	Not Active	Predicted SARS-Cov-2 Protease inhibitor	Anticonvulsants	Sigma Aldrich
	Laflunimus Sodium Salt	Not Active	Predicted SARS-Cov-2 Protease inhibitor	Anti-inflammatory	Quimigen

Supplementary Table 4

ACTIVITY	DRUG	IC_{50} / CC_{50} µM (Mean +/-SD)	Mode of Action	Previous Clinical Use	Vendor Origen
UNKNOWN	Azithromycin (Zitromax)	Not Active / > 100	Antibiotic	Bacteria	Pfizer
	Doxycycline (Anaclosil)	Not Active / > 100	Antibiotic	Bacteria	Reig
	Eravacycline (Xerava)	Not Active / > 4	Antibiotic	Resistent bacteria	Tetraphase Pharmaceuticals
	Quinacrine dihydrochloride	Not Active / > 6	Inhibitor of NF-kappaB	Parasites	Sigma Aldrich
	Ivermectin (Stromectol)	Not Active / > 2	Nuclear import inhibitor	Parasites	MSD
	Mefloquine hydrochloride	Not Active / > 100	Phospholipid bilayer?	Malaria	Sigma Aldrich
	N-Acetil cystein (Flumil)	Not Active / > 100	Synthesis of glutathione	Influenza	Zambon
	Itraconazole	79.37 / > 100	Inhibits OSBP, which produces the membrane-bound viral replication organelles	Fungus	Janssen
	Fluconazol	Not Active / > 100	Antibiotic	Fungus	Franesius Kabi
	Famotidine	Not Active/ > 100	Histamine-2 receptor antagonist	Gastric	Normon
	Cetirizine dihydorcloride	Not Active/ > 100	Histamine-H1 receptor antagonist	Antihistaminic	Sigma Aldrich
	Colchicine	Not Active / 0.63	Anti mytotic	Gout attacks	Merck
	Palbociclib	Not Active/ 2,7	CDK4/6 inhibitor	Breast cancer	Selleckchem
	Ribociclib	Not Active / > 20	CDK4/6 inhibitor	Breast cancer	Selleckchem
	Abenaciclib	Not Active / > 1	CDK4/6 inhibitor	Breast cancer	Selleckchem
	Silibinin	Not active / > 20	?	Liver disease	Rottapharm Madaus
	Atorvastatin	Not active / > 20	HMG-CoA reductase inhibitor	Cardiovascular disease	Normon
	Fenofibrate	19.8 +/- 8 / > 100	Activates PPARα	Dyslipidemia	Lacer
	MDL 28170	0.14 +/- 0.06 / > 87	Calpain III inhibitor & Cathepsin B inhibitor	*Pre-Clinical*	Merck
	NPO-2142; -2143 & -2260	~ 0.54 / > 10	Calpain & Cathepsin inhibitors	*Pre-Clinical*	Landsteiner Genmed
	NPO-2138	*Not calculated, but partially active at 100* / > 10	Calpain & Cathepsin inhibitors	*Pre-Clinical*	Landsteiner Genmed

Supplementary Table 5